Çukurova Üniversitesi Mühendislik Mimarlık Fakültesi Dergisi, 35(1), ss. 139-147, Mart 2020
Çukurova University Journal of the Faculty of Engineering and Architecture, 35(1), pp. 139-147, March 2020

Heat Conduction Analysis of Two-Dimensional Anisotropic Plate

Durmuş YARIMPABUÇ[1], Ertuğrul CİHAN[2], Kerimcan ÇELEBİ[*3], Mehmet EKER[2]

[1]Osmaniye Korkut Ata Üniversitesi, Fen Edebiyat Fakültesi, Matematik Bölümü, Osmaniye
[2]Osmaniye Korkut Ata Üniversitesi, Mühendislik Fakültesi, Makine Mühendisliği Bölümü, Osmaniye
[3]Çukurova Üniversitesi, Ceyhan Mühendislik Fakültesi, Makine Mühendisliği Bölümü, Adana

Geliş tarihi: 20.02.2020 *Kabul tarihi: 15.05.2020*

Abstract

The heat conduction of a two dimensional anisotropic plate with non-homogeneous general boundary conditions is solved by using ANSYS Fluent in the cartesian coordinate system. It is assumed that the thermal conductivity and heat generation of the material arbitrarily change in the direction of the two space variables. Under these conditions, a variable coefficient differential equation is obtained. Analytical solutions of such equations cannot be obtained except for some simple material functions. The variable coefficient differential equation, which includes the heat conduction coefficient and volumetric heat generation depending on the two space variables and non-homogeneous boundary conditions, is handled numerically by ANSYS Fluent user-defined function (UDF). The accuracy of the numerical method is demonstrated by comparing analytical and numerical solutions using simple material functions.

Keywords: Anisotropic heat conduction, Analytical solution, Finite element method, UDF

İki Boyutlu Anizotropik Plakanın Isı İletim Analizi

Öz

Homojen olmayan genel sınır koşullarına sahip iki boyutlu anizotropik bir plakanın ısı iletim problemi, kartezyen koordinat sisteminde ANSYS Fluent kullanılarak çözülmüştür. Malzemenin termal iletkenliği ve ısı üretiminin keyfi olarak iki uzay değişkeni yönünde değiştiği varsayılmıştır. Bu koşullar altında sistemi modelleyen değişken katsayılı diferansiyel denklem elde edilir. Bu tür denklemlerin analitik çözümleri, bazı basit malzeme fonksiyonları dışında elde edilemez. İki uzay değişkenine bağlı olarak değişen ısı iletim katsayısı ve hacimsel ısı üretimi ile homojen olmayan sınır koşullarını içeren değişken katsayılı diferansiyel denklem ANSYS Fluent kullanıcı tanımlı fonksiyon (UDF) ile sayısal olarak ele alınmıştır. Sayısal yöntemin doğruluğu, basit malzeme fonksiyonları kullanılarak analitik ve sayısal çözümler karşılaştırılarak gösterilmiştir.

Anahtar kelimeler: Anizotropik Isı iletimi, Analitik çözüm, Sonlu elemanlar yöntemi, UDF

[*]Sorumlu (Corresponding author) yazar: Kerimcan ÇELEBİ, *kcelebi@cu.edu.tr*

1. INTRODUCTION

Anisotropic materials whose material properties change with the direction can be natural and synthetic such as, crystals, wood, sedimentary rocks, metals that have undergone heavy cold pressing, laminated sheets, cables, heat shielding materials for space vehicles and fiber reinforced composite structures. In aforementioned materials, thermal conductivity can change with the location of the material as well. The change in material properties such as thermal conductivity depends on the location throughout the medium are also examples of anisotropic materials which results in governing differential equations with variable coefficients. Due to the difficulties associated with the solution of these heat transfer problems with variable coefficients, simplifying assumptions are usually made. For example, in the case of materials that have thermal conductivity which varies slightly with location, constant thermal conductivity is generally assumed. This assumption leads errors in solution if the thermal conductivity of the material is affected greatly with location change throughout the material. Therefore, modelling and simulating temperature distribution for such problems linearities caused by location-dependent thermal conductivity have to be accounted by the numerical computation.

There are various methods available in the literature to handle heat transfer problems with variable coefficients. The most commonly used engineering methods are Finite Difference Method (FDM) [1] and Finite Element Methods (FEM) [2]. The biggest advantage FEM over the FDM is its capability of handling irregular geometries and size can be changed over the region. Another method usually utilized in this kind of analyses is the (Boundary Element Method) BEM [3]. In this method the numerical solution of the continuum is performed with a reduction of dimensionality of the problem. The efficiency of BEM is that the number of the resulting simultaneous equations depends only upon the discretization of the boundary of the domain and that technique can be employed to represent the solution over the boundary elements. In this way, the problem can be treated with one less dimension. The most common used engineering solution for the linear heat transfer problem is FEM.

Ma et al. [4] and [5] have proposed an analytical solution of heat conduction problem for an anisotropic medium; they employed a linear transformation to convert the original anisotropic problem to an equivalent isotropic problem with a same geometrical configuration. The accuracy improvement of the discontinuous boundary elements over the continuous boundary elements has been well established numerically in Mera et al [6], Florez and Power [7] and Tadeu and Antonio [8]. The anisotropy increases the number of heat conduction constants, which renders the derivation of fundamental solutions as difficult even in a homogeneous case. Sladek et al. [8] proposed the meshless method based on the local Petrov-Galerkin approach to solve stationary and transient heat conduction problems in 2-D for anisotropic FGM. Wang et al. [9] developed a new meshless method based on the standard Laplacian operator and radial basis functions (RBFs) in order to solve steady-state heat conduction problems with arbitrarily spatially varying thermal conductivity in isotropic and anisotropic materials.

In the scientific literature, many analytical works have focused on relevant anisotropic heat conduction problems. A linear coordinate transformation is well-known as it can be applied to solve the heat conduction problems for a thin-layer medium and multi-layered media with anisotropic properties [11-16]. The effect of the contact resistance on the steady-state temperature in a multidimensional and multilayer body was studied by Haji-Sheikh et al. [12]. However, analytical treatments have been restricted within quite special or simple cases, because of the solution, especially for more complex geometry, poses mathematical difficulties. The boundary element method (BEM) was used for solving the multidimensional and multilayer anisotropic heat conduction problem by adopting the direct domain mapping and the coordinate transforms method [13]. The advantage of this approach is that the anisotropic problem can be efficiently and accurately solved with any numerical methods in the literature, such as the finite difference method or the boundary element method for isotropic potential theory [14-16]. The coordinate transforms method can also efficiently be used for analysis of the anisotropic microscale heat transfer.

In this paper, numerical method with location dependent heat source and non-homogeneous boundary condition fields was extended to obtain solution of anisotropic linear heat transfer problems with variable coefficients. This study involved development and implementation of numerical algorithms and software. The research is focused on governing differential equations with variable coefficients caused by location dependency of thermal conductivity and volumetric heat generation. Analytical solution for simple material functions available in literature [17] are used to validate the numerical model.

2. GOVERNING EQUATION

Two-dimensional steady state conduction in a rectangular plate L×W at a uniform volumetric rate is considered for the thermal conductivity and energy generation varies arbitrary in two spatial directions shown in Figure 1.

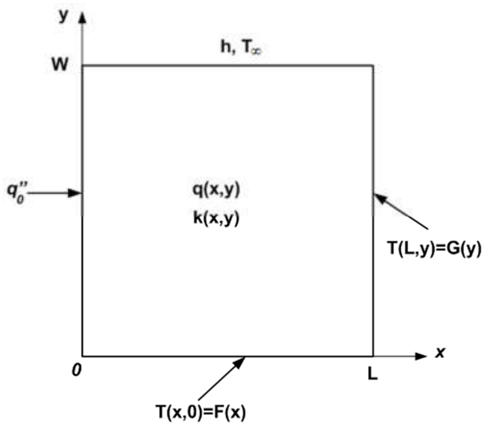

Figure 1. The geometry of 2D steady state conduction in a rectangular plate L×W

This non-homogeneous second order partial differential equation with variable coefficient is governed by Equation 1.

$$\frac{\partial}{\partial x}\left(k(x,y)\frac{\partial T}{\partial x}\right)+\frac{\partial}{\partial y}\left(k(x,y)\frac{\partial T}{\partial y}\right)+q(x,y) = 0 \quad (0<x<L, 0<y<W) \tag{1}$$

with nonhomogeneous boundary conditions Equation 2:

$$\frac{\partial T}{\partial x}(0,y)=\frac{\dot{q}_0}{k(x,y)};\quad T(L,y)=G(y),$$
$$T(x,0)=F(x);\quad \frac{\partial T}{\partial y}(x,W)=-\frac{h}{k(x,W)}\left[T(x,W)-T_\infty\right] \tag{2}$$

where k(x,y),q(x,y) thermal conductivity and heat generation respectively. In the treatment, functions of spatial variables in three different case are assumed.

Case-1: Thermal conductivity and heat generation are varied exponentially in one spatial variables Equation 3a,

$$k(y)=k_0e^{-\gamma\frac{y}{W}},q(y)=q_0e^{-\gamma\frac{y}{W}} \tag{3a}$$

Case-2: Thermal conductivity and heat generation are varied exponentially in two spatial variables, Equation 3b,

$$k(x,y)=k_0e^{\alpha\frac{x}{L}}e^{-\gamma\frac{y}{W}},q(x,y)=q_0e^{\beta\frac{x}{L}}e^{-\gamma\frac{y}{W}} \tag{3b}$$

Case-3: Thermal conductivity and heat generation are varied exponentially and in power law, respectively in two spatial variables Equation 3c,

$$k(x,y)=k_0e^{-\gamma\frac{x}{L}}e^{-\gamma\frac{y}{W}},q(x,y)=q_0x^3(1-x)y^3(1-y) \tag{3c}$$

where, k_0 and q_0 are the thermal conductivity and internal heat generation at the ambient temperature, T_∞. And, α,β,γ represents the variations of the thermal conductivity and internal heat generation.

For simple representation, it is assumed that thermal conductivity and heat generation are varied exponentially in one spatial direction (Case-1). Therefore, the governing equation by using the following dimensionless variables Equation 4,

$$\eta=\frac{x}{L},\xi=\frac{y}{W},\theta=\frac{T-T_\infty}{T_{max}-T_\infty} \quad (4)$$

renders eq. (1) in the form of nonhomogeneous ordinary differential equations with constant coefficients Equations 5 and 6,

$$\frac{\partial^2\theta}{\partial\eta^2}-c^2\gamma\frac{\partial^2\theta}{\partial\xi}+c^2\frac{\partial\theta}{\partial\xi^2}+d=0(0<\eta<1,0<\xi<1) \quad (5)$$

where

$$c=\frac{L}{W},d=\frac{q_0L^2}{k_0(T_{max}-T_\infty)} \quad (6)$$

The non-dimensional nonhomogeneous boundary conditions turned into the following form Equations 7 and 8,

$$\frac{\partial\theta}{\partial\eta}(0,\xi)=-ae^{\gamma\xi}; \quad \theta(1,\xi)=g(\xi),$$
$$\theta(\eta,0)=f(\eta); \quad \frac{\partial\theta}{\partial\xi}(\eta,1)=-e^{\gamma}B_i\theta(\eta,1) \quad (7)$$

with

$$Bi=\frac{hL}{k_0},a=\frac{q_0^{''}L}{k_0(T_{max}-T_\infty)}. \quad (8)$$

where Bi is the Biot number. It is emphasized that the main aim of this paper is to obtain numerical solution of two dimensional thermal conduction equation with the given most general nonhomogeneous boundary conditions.

3. NUMERICAL METHOD

The governing partial differential equation mentioned earlier is solved by using the commercially available ANSYS FLUENT software. The foundation of physical problem, meshing the domain and application of the boundary conditions are all done with the preprocessor of the same software ANSYS ICEM CFD. It is well-known that the aforementioned software utilizes the widely used finite element and finite volume modeling for the heat transfer and mechanics. The results are comprehended in the post processor module of the ANSYS Workbench CFD software.

Although the ANSYS FLUENT is very capable of solving physical problems, in some cases the standard interface cannot be programmed to address the problems with complicate boundary conditions and variable parameters such as the problem studied in this paper. Due to the customized boundary conditions presented in this paper, a User Defined Function [19] is inevitable to be employed for numerical solution. The UDF is a C routine programmed by the user which can be dynamically linked with the solver. The conduction differential equation with location dependent heat conduction coefficient, volumetric heat generation and nonhomogeneous boundary conditions require the employment of UDFs by developing codes in C. The simultaneous processing of the UDFs with FLUENT model deploys accurate results for the demanded boundary temperature profile and the heat flux. The input parameters for UDFs were taken as $\alpha=2$, $\beta=4$, $\gamma=0.5$, $L=0.2$, $W=0.2$, $T_{max}=500$, $T_\infty=300$, $k_0=0.2$.

3.1. Mesh Sensitivity Analysis

The numerical solutions are run for five different mesh densities to examine the mesh sensitivity of the described simulations. The mesh is refined by increasing the number of divisions of edges of the body in x and y directions. In this study, the edges of the body are divided by 10x10, 20x20, 40x40, 80x80, 160x160 and 320x320 in order to analyze the mesh sensitivity of the problem by comparing the heat transfer results at the top (ξ=1) boundary. The results are monitored in Table 1. A maximum residual reduction factor of 10^{-9} for the heat conduction equation was used to monitor the convergence of iterative solution. The discretization error in the numerical solutions is calculated in the following form [18] (Equation 9).

$$\varepsilon_h \approx \frac{\O_h-\O_{2h}}{2^p-1} \quad (9)$$

The order of the scheme coefficient p in eq.(20) is given by following relation (Equation 10):

$$p = \frac{\log\left(\frac{\O_{2h} - \O_{4h}}{\O_{h} - \O_{2h}}\right)}{\log(2)} \quad (10)$$

The Richardson extrapolation suggests that an approximation of the exact solution ϕ is more accurate than the solution of the finest mesh $\O_h$ by adding the discretization error ϵ_h. The approximation of exact solution is expressed as following (Equation 11):

$$\phi = \O_h + \epsilon_h \quad (11)$$

The relative discretization error is given in the Equation 12 below and calculated by the heat flux given in Table 2.

$$\Psi(\%) = \frac{\varepsilon_h}{\O_h + \varepsilon_h} \times 100. \quad (12)$$

Table 1. Q(W/m^2), the amount of heat transferred at the top ($\xi = 1$) boundary

n	Number of Cell	"Bi=1"	Bi=5	Bi=10	Bi=30	Bi=60
10×10	100	222.14	376.53	416.37	449.38	458.78
20×20	400	224.33	390.94	434.12	470.20	480.59
40×40	1600	225.07	398.69	443.82	481.68	492.64
80×80	6400	225.45	402.87	449.09	487.95	499.25
160×160	25600	225.65	405.07	451.87	491.28	502.76
320×320	102400	225.75	406.19	453.29	492.98	504.56
Analytical	225.90	407.39	454.85	495.25	507.09	

Table 2. Relative discretization error for a=1.5 and d=5 at the top (ξ=1) boundary

	Bi=1	Bi=5	Bi=10	Bi=30	Bi=60
$\O_h$	225.75	406.19	453.29	492.98	504.56
p	1.1171	0.9721	0.9678	0.9687	0.9624
ε_h	0.0814	1.1648	1.4863	1.7786	1.9005
Φ	225.83	407.35	454.77	494.76	506.47
Ψ(%)	0.03603	0.2859	0.3268	0.3595	0.3752

4. RESULTS AND DISCUSSION

The temperature distribution for the case that thermal conductivity and volumetric heat generation are varied exponentially in one spatial variables are presented in Figure 2-7. In these figures, the results obtained in the numerical results are compared with the analytical study of Yarımpabuç et al. [17], and It can be seen from Figure 2-7 that the numerical results are in a good agreement with the analytical results and both solutions satisfy boundary conditions imposed in the problem.

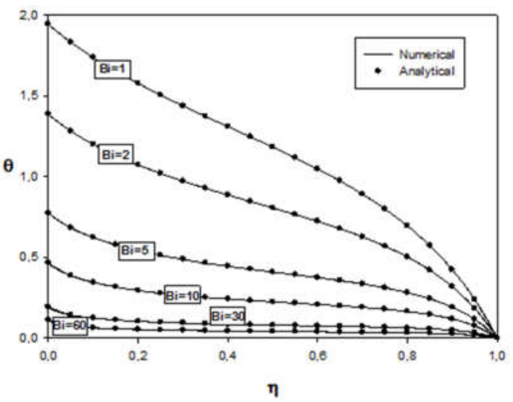

Figure 2. Dimensionless temperature distribution for different Biot number at the top (ξ=1) boundary

The variation of temperature in the body for various Bi numbers is displayed in Figure 2–3 with a=1.5 and d=5. In Figure 2 numerical and analytical solutions are presented for different values of Bi=1, 2, 5, 10, 30 and 60. The numerical and analytical solutions are coinciding accurately for all the Bi numbers. As the Biot number increases the heat transfer increases yielding the temperature on top wall to approach the ambient temperature. On the other hand, temperature of the same wall increases due to the volumetric heat generation and heat flux while Bi number is decreasing. However at point (η=1, ξ=1) the temperature is found to be $\theta = 0$ which satisfies the BC's described in problem definition for all Bi numbers. It is also shown that dimensionless temperature value approaches to zero as Bi number goes to infinity.

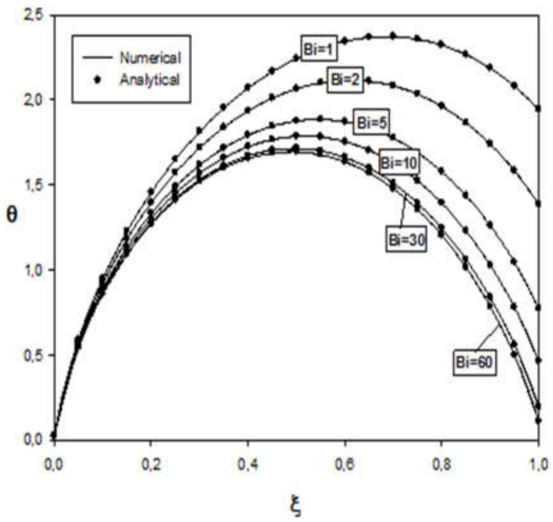

Figure 3. Dimensionless temperature distribution for different Biot number at the left (η=0) boundary

The dimensionless temperature distribution along left wall ($\eta = 0$) for Bi = 1, 2, 5, 10, 30 and 60 with constans values of a=1.5 and d=4 is provided in Figure 3. It is clearly seen that dimensionless temperature θ becomes $\xi = 0$ which is expected because it is imposed as the boundary condition in the problem definition. The dimensionless temperature θ distribution tends to have lower value while Bi number increases.

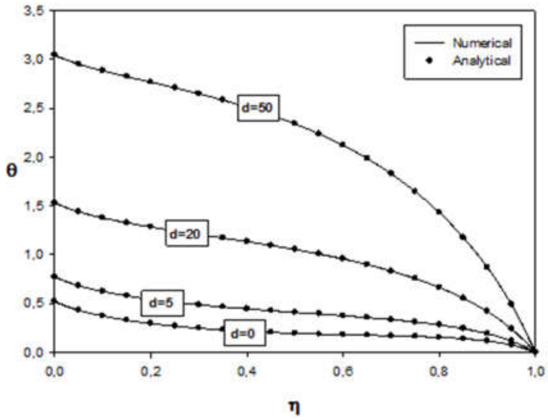

Figure 4. Dimensionless temperature distribution at the top (ξ=1) boundary

The change of dimensionless temperature distributions for assorted dimensionless volumetric heat generation values d=0, 5, 20 and 50 with Bi=5 and a=1.5 is shown in Figure 4-5. In Figure 4, the temperature distribution of the medium considerably increases as the volumetric heat generation increases. However, when volumetric heat generation is neglected (d=0) in the medium, temperature seems not to be affected substantially for Bi=5 and a=1.5.

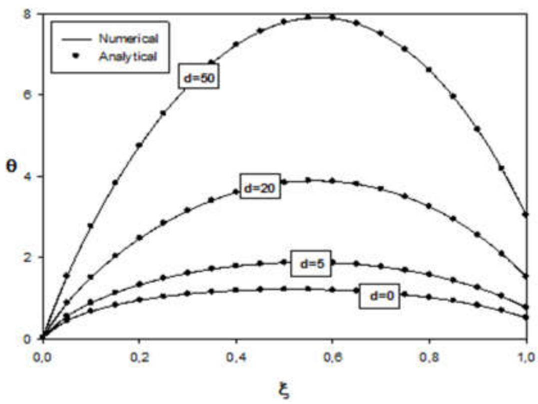

Figure 5. Dimensionless temperature distribution at the left (η=0) boundary

In Figure 5, the temperature distributions along left wall (η = 0) with constant Biot number Bi=5 and dimensionless heat flux a=1.5 for dimensionless volumetric heat generations d=0, 5, 20 and 50 are illustrated. The temperature along the wall increases remarkably as the volumetric heat generation is increased with constant heat flux. Similar to Figure 3 the temperature along the wall reaches to a maximum and then decreases. According to Figure 5 the maximum temperature value happens to be at the middle of the wall. The temperature alters slightly when heat generation is not deployed.

Effect of dimensionless heat flux (a=0, 0.25, 0.5, 1.0, 1.5) on temperature for constant Bi number (Bi=5), volumetric heat generation (d=5) is plotted in Figure 6-7.

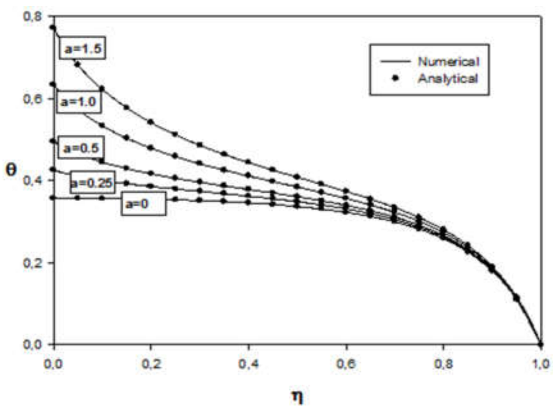

Figure 6. Dimensionless temperature distribution at the top (ξ=1) boundary

In Figure 6, the temperature distribution on top wall ($\xi = 1$) decreases as the heat flux value decreases. The temperature does not differ along the wall of interest when the heat flux does not exist. Similar to the other plots, the temperature $\xi = 1$ vanishes to zero satisfying the enforced boundary conditions. It is shown that the volumetric heat generation dominates the temperature distribution along the top wall over the heat flux. The temperature distribution for the left wall for numerous dimensionless heat flux (a= 0, 0.25, 0.5, 1.0, 1.5) is plotted in Figure 7 for constant Bi number (Bi= 5) and volumetric heat generation (d= 5). According to the figure, the temperature distribution on the wall tends to shift upward as the heat flux is increased. The temperature θ becomes zero assuring the boundary conditions employed in the problem definition $\xi = 0$. However at $\xi = 1$, the dimensionless temperature values depend on the Biot number employed on the top wall. The temperature at $\xi = 1$ is anticipated to become zero approaching to the ambient temperature.

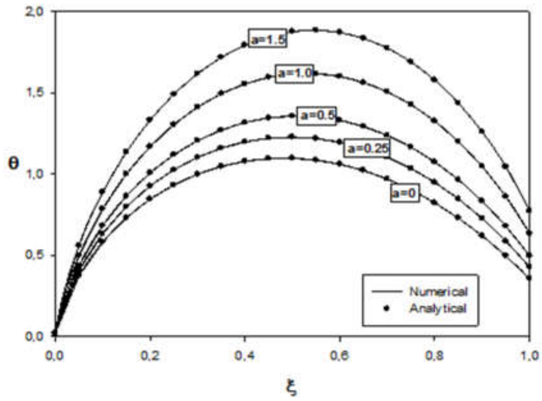

Figure 7. Dimensionless temperature distribution at the left (η= 0) boundary

In Figure 8-9, the results of numerical solution of the problem for the case that thermal conductivity and volumetric heat generation are varied exponentially in two spatial variables. The dimensionless temperature distribution of the top ($\xi = 1$) and left wall ($\eta = 0$) with respect to the Bi number for a constant a= 1.5 and d= 5 is provided in Figure 8 and 9 respectively. According to results presented in Figure 8, the temperature of the top wall approaches to ambient temperature for higher Bi numbers. Similarly, in Figure 9 the temperature distributions of the left wall increase as the Bi number decreases due to decrease of the heat transfer from wall to the environment.

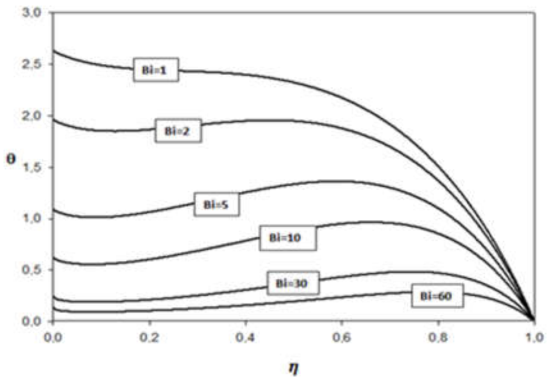

Figure 8. Dimensionless temperature distribution at the top (ξ= 1) boundary

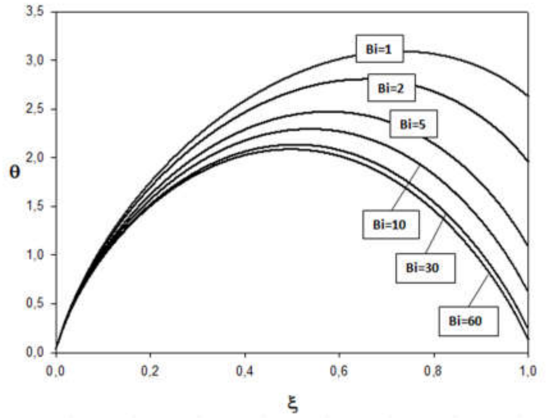

Figure 9. Dimensionless temperature distribution at the left (η= 0) boundary

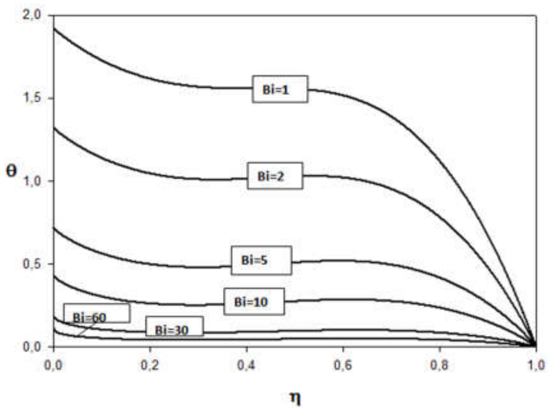

Figure 10. Dimensionless temperature distribution at the top (ξ= 1) boundary

In addition, the results of numerical solution of the problem for the case that thermal conductivity changed exponentially, and internal heat generation changed with power law in two spatial variables are presented in Figure 10-11. The dimensionless temperature distribution of the top and left wall with respect to the *Bi* number for a constant *a*= 1.5 and d= 5 is provided in Figure 10 and 11 respectively. According to results presented in Figure 10, as Bi number increases, the temperature of the top wall comes close to the ambient temperature. Furthermore, in Figure 11 the temperature of the left wall increases as the Bi number decreases due to developing resistance against heat transfer from wall to the environment.

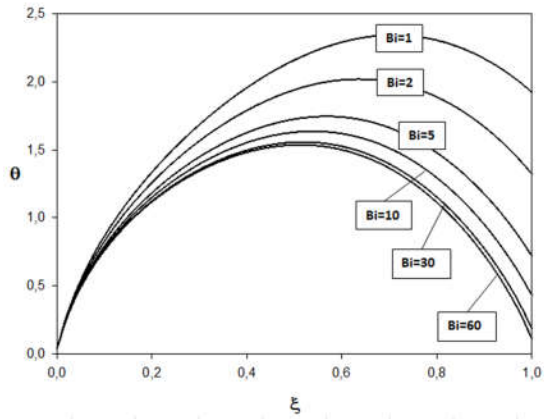

Figure 11. Dimensionless temperature distribution at the left (η= 0) boundary

5. CONCLUSION

In this study heat conduction equation of an anisotropic medium with location dependent heat generation and nonhomogeneous boundary conditions is solved numerically. The numerical solution of the defined problem is performed in the commercially available software ANSYS Fluent. The heat conduction coefficient, location dependent heat generation and nonhomogeneous boundary conditions are imposed by the help of ANSYS Fluent UDF.

The results obtained agree with analytical solution remarkably. The error margin remains to be in the vicinity of 0.5%. The temperature distributions of the model for dimensionless numbers are explored and they are consistent with each other. According to the results presented, the temperature distribution is governed greatly by the heat generation rather than heat flux. The proposed models are capable of solving and analyzing of heat conduction equations for different and anisotropic materials.

6. REFERENCES

1. Zedan, M., Schneider, G.E., 1982. A Physical Approach to the Finite-difference Solution of the Conduction Equation in Generalized Coordinates, Num.H Trans., Part A, 5(1), 1-19.

2. Comini, G., Guidice, S., Lewis, R.W., Zienkiewicz, O.C., 1974. Finite Element Solution on Nonlinear Heat Conduction Problems with Special Reference to Phase Change, Int. J. for Num. Methods in Eng., 8, 613-624.

3. Wrobel, L.C., Aliabadi, M.H., 2002. The Boundary Element Method: Applications in Solids and Structures, 2 Volume Set, John Wiley and Sons, USA, 1066.

4. Hsieh, M.H., Ma, C.C., 2002. Analytical Investigations for Heat Cond. Prob. in Anisotropic Thin-layer Media with Embedded Heat Sources, Int.J.H.M.Trans., 45(20), 4117-4132.

5. Ma, C.C., Chang, S.W., 2004. Analytical Exact Solutions of Heat Conduction Problems for Anisotropic Multi-layered Media, Int. J. Heat Mass Trans., 47(8-9), 1643–1655.

6. Mera, N.S., Elliot, L., Ingham, D.B., Lesnic, D., 2001. A Comparison of Boundary Element Method Formulations for Steady State Anisotropic Heat Conduction Problems, Eng. Anal. Bound. Elem., 25(2), 115–28.

7. Florez, W.F., Power, H., 2001. Comparison Between Continuous and Discontinuous Boundary Elements in the Multidomain Dual Reciprocity Method for the Solution of the Two-dimensional Navier-Stokes Equations, Eng. Anal. Bound. Elem., 25(1), 57–69.

8. Tadeu, A., Antonio, J., 2000. Use of Constant, Linear and Quadratic Boundary Elements in 3D Wave Diffraction Analysis, Eng. Anal. Bound. Elem., 24(2), 131–144.

9. Wang, H., Qin, Q.H., Kang, Y.L., 2005. A New Meshless Method for Steady-state Heat Conduction Problems in Anisotropic and Inhomogeneous Media, Arc. App. Mech., 74(8), 563–579.

10. Sladek, J., Sladek, V., Atluri, S.N., 2004. Meshless Local Petrov-Galerkin Method for Heat Conduction Problem in an Anisotropic Medium, CMES, Comput Model Eng. Sci., 6(3), 309–318.

11. Hsieh, M.H., Ma, C.C., 2002. Analytical Investigations for Heat Conduction Problems in Anisotropic Thin-layer Media with Embedded Heat Sources, Int.J.H.M.Trans., 45(20), 4117-4132.

12. Haji-Sheikh, A., Beck, J.V., Agonafer, D., 2003. Steady-state Heat Conduction in Multi-layer Bodies, Int. J. Heat Mass Transfer, 46(13), 2363–2379.

13. Shiah, Y.C., Tan, C.L., 1997. BEM Treatment of Two-dimensional Anisotropic Field Problems by Direct Domain Mapping, Engineer. Anly. Bound. Element, 20(4), 347-351.

14. Shiah, Y.C., Tan, C.L., 2004. BEM Treatment of Three-dimensional Anisotropic Field Problems by Direct Domain Mapping, Engineer. Anly. Bound. Element, 28(1), 43–52.

15. Shiah, Y.C., Hwanh, P.W., Yang, R.B., 2006. Heat Conduction in Multiply Adjoined Anisotropic Media with Embedded Point Heat Sources, J. Heat Transfer, 128(2), 207–214.

16. Shiah, Y.C., Lee, B.J., 2011. Boundary Element Modeling of 3-D Anisotropic Heat Conduction Involving Arbitrary Volume Heat Source, Math.Comp.Mod., 54(9-10), 2392-2402.

17. Yarımpabuç, D., Cihan, E., Eker, M., Celebi, K., 2016. Analytical and Numerical Solutions of Anisotropic Heat Conduction Problems with Location-dependent Heat Generation, 1st International Mediterranean Science and Engineering Congress (IMSEC 2016), 1673-1680, Paper ID:496.

18. Ferziger, J.H., Peric, M., 2002. Computational Methods for Fluid Dynamics, Third Ed. Springer, 431, USA.

19. ANSYS, Inc., 2009. Ansys Fluent 12.0 UDF Manual, 2070.